An Observational Perspective of Low Mass Dense Cores II: Evolution towards the Initial Mass Function

Derek Ward-Thompson

Cardiff University

Philippe André

Service d'Astrophysique de Saclay

Richard Crutcher

University of Illinois

Doug Johnstone

National Research Council of Canada

Toshikazu Onishi

Nagoya University

Christine Wilson

McMaster University

We review the properties of low mass dense molecular cloud cores, including starless, prestellar, and Class 0 protostellar cores, as derived from observations. In particular we discuss them in the context of the current debate surrounding the formation and evolution of cores. There exist several families of model scenarios to explain this evolution (with many variations of each) that can be thought of as a continuum of models lying between two extreme paradigms for the star and core formation process. At one extreme there is the dynamic, turbulent picture, while at the other extreme there is a slow, quasi-static vision of core evolution. In the latter view the magnetic field plays a dominant role, and it may also play some role in the former picture. Polarization and Zeeman measurements indicate that some, if not all, cores contain a significant magnetic field. Wide-field surveys constrain the timescales of the core formation and evolution processes, as well as the statistical distribution of core masses. The former indicates that prestellar cores typically live for 2–5 free-fall times, while the latter seems to determine the stellar initial mass function. In addition, multiple surveys allow one to compare core properties in different regions. From this it appears that aspects of different models may be relevant to different star-forming regions, depending on the environment. Prestellar cores in cluster-forming regions are smaller in radius and have higher column densities, by up to an order of magnitude, than isolated prestellar cores. This is probably due to the fact that in cluster-forming regions the prestellar cores are formed by fragmentation of larger, more turbulent cluster-forming cores, which in turn form as a result of strong external compression. It is then the fragmentation of the cluster-forming core (or cores) that forms a stellar cluster. In more isolated, more quiescent, star-forming regions the lower ambient pressure can only support lower density cores, which go on to form only a single star or a binary/multiple star system. Hence the evolution of cluster-forming cores appears to differ from the evolution of more isolated cores. Furthermore, for the isolated prestellar cores studied in detail, the magnetic field and turbulence appear to be playing a roughly equal role.

1. INTRODUCTION

A great deal is now known about dense cores in molecular clouds that are the progenitors of protostars – see the previous chapter by *Di Francesco et al.*, which details many of the observational constraints that have been placed upon their physical parameters (this chapter and the preceding chapter should be read in conjunction). What is less clear is the manner in which the cores are formed and subsequently evolve. In this chapter we discuss what the observations can tell us about the formation and evolution of cores. Clearly the evolution depends heavily upon the formation mech-
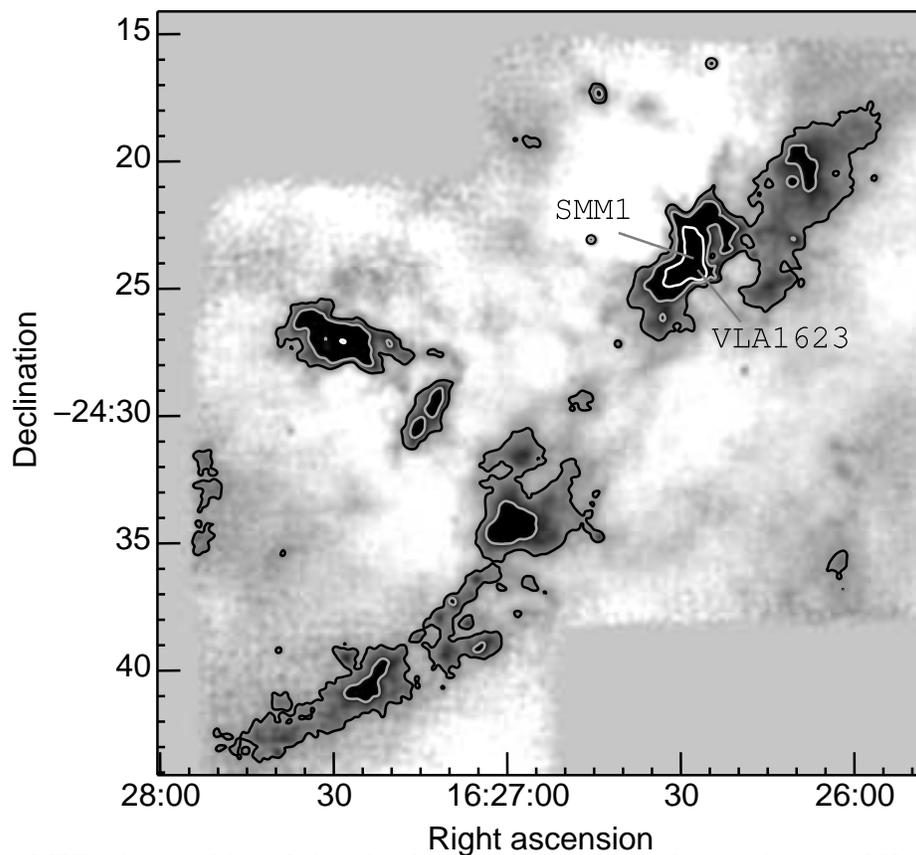
Fig. 1.— SCUBA image of the ρ Oph molecular cloud region seen in dust continuum at 850 μm (adapted from *Johnstone et al.*, 2000). Prestellar, protostellar and cluster-forming cores can all be seen in this molecular cloud region. For example, the cluster-forming core ρ Oph A (extended region in the upper right of this image) contains within it (inside the white contour) the prestellar core SM1 and Class 0 protostellar core VLA1623 (cf. *André et al.*, 1993). Note also that large areas of the cloud contain no dense cores, leading to the idea of a threshold criterion discussed in Section 6.

anism, and upon the dominant physics of that formation. Several model scenarios have been proposed for this mechanism.

These models can be thought of as a small number of families of models, each of which contains many variations, representing a continuum lying between two extremes. At one extreme there is a school of thought that proposes a slow, quasi-static evolution, in which a core gradually becomes more centrally condensed. This evolution may be moderated by the magnetic field (e.g., *Mouschovias and Ciolek*, 1999) or else by the gradual dissipation of low-level turbulent velocity fields (e.g., *Myers*, 1998, 2000). At the other extreme is a very dynamic picture (e.g., *Ballesteros-Paredes et al.*, 2003), in which highly turbulent gas creates large density inhomogeneities, some of which become gravitationally unstable and collapse to form stars (for a review, see: *Ward-Thompson*, 2002). Once again the magnetic field may play a role in this latter picture, in which magneto-hydrodynamic (MHD) waves may be responsible for carrying away excess turbulent energy (e.g., *Ostriker et al.*, 1999).

What we find from the observations is that some aspects of each of these different model scenarios may be relevant in different regions of star formation, depending on the local environment. No two regions are the same, and the effects of local density, pressure and magnetic field strength, and the presence or absence of other nearby stars and protostars all play an important role in determining what dominates the formation and evolution of dense molecular cloud cores.

Throughout this chapter we define a dense core as any region in a molecular cloud that is observed to be significantly over-dense relative to its surroundings. We define a starless core as any dense core that does not contain any evidence that it harbours a protostar, young stellar object or young star (*Beichman et al.*, 1986). Such evidence would include an embedded infra-red source, centimetre radio source or bipolar outflow, for example (cf. *André et al.*, 1993, 2000).

Any core that does contain such evidence we define as a protostellar core. This might be a Class 0 protostellar core (*André et al.*, 1993, 2000) or a Class I protostellar core (*Lada*, 1987; *Wilking et al.*, 1989) depending upon its evolutionary status.

We here define prestellar cores (formerly pre-protostellar cores – *Ward-Thompson et al.*, 1994) as that subset of starless cores which are gravitationally bound and hence are expected to participate in the star formation process. We further define cluster-forming cores as those cores that have significant observed structure within them, such that they appear to be forming a small cluster or group of stars rather than a single star or star system. Examples of the various types of cores can be seen in Figure 1.

We note that the resolution of current single-dish telescopes is insufficient in more distant regions to differentiate between cluster-forming cores and other types of core. Hence we restrict most of our discussion to nearby molecular clouds – typically we restrict our discussion to d < 0.5 kpc.

2. EVOLUTIONARY MODELS

We begin by summarising some of the key model parameters and predictions. One such discriminator between the extreme pictures mentioned above is the timescale of core evolution. Therefore we first discuss some predictions of the models regarding core lifetimes.

If turbulent dissipation in a quasi-static scenario is the relevant physics, then the timescale of the dissipation of turbulence could be several times the free-fall time (e.g., *Nakano*, 1998). However, if highly turbulent processes dominate molecular cloud evolution then detailed modelling yields results which suggest that cores only live for approximately one or two free-fall times (e.g., *Ballesteros-Paredes et al.*, 2003; *Vazquez-Semadeni et al.*, 2005).

In the magnetically-dominated paradigm, molecular clouds may form by accumulation of matter along flux tubes, by (for example) the Parker instability (*Parker*, 1966). Furthermore, if magnetic fields dominate the evolution then a key parameter is the ratio of core mass to magnetic flux (M/Φ). A critical cloud or core is defined as one in which the energy density of the magnetic field exactly balances the gravitational potential energy.

For clouds with magnetic fields stronger than is necessary for support against gravitational collapse, M/Φ is subcritical; for fields too weak to support clouds, M/Φ is supercritical. Consequently, two possible extreme-case scenarios arise: one in which low-mass stars form in originally highly magnetically subcritical clouds, with ambipolar diffusion leading to core formation and quasi-static contraction of the cores (e.g., *Mouschovias*, 1991; *Shu et al.*, 1987); and the other in which clouds are originally supercritical (e.g., *Nakano*, 1998). In the absence of turbulent support, highly supercritical collapse occurs on essentially the free-fall time.

Since magnetic fields can be frozen into only the ionized component of clouds, neutral matter can be driven by gravity through the field. Hence, if a star is formed in an originally very magnetically subcritical cloud, the relevant timescale is the ambipolar diffusion timescale, τ_{AD}, which is proportional to the ionisation fraction X_e. This is normally taken to have a power-law dependence on density: $\tau_{AD} \propto X_e \propto n(\mathrm{H}_2)^{-0.5}$ for $A_V > 4$, where cosmic-ray ionisation dominates (*McKee*, 1989; *Mouschovias*, 1991). For $A_V < 4$ UV ionisation dominates, leading to a steeper dependence (*McKee*, 1989), but this regime is not believed to be significant for prestellar cores.

Since τ_{AD} is shorter in denser regions, the process of ambipolar diffusion increases M/Φ in overdense regions of the cloud, leading to the formation of cores. Eventually, M/Φ is increased from subcritical to supercritical and the core collapses. For highly subcritical clouds τ_{AD} is roughly ten times the free-fall time (*Nakano*, 1998), although *Ciolek and Basu* (2001) point out that the ambipolar diffusion timescale of marginally subcritical cores within clouds can be as little as a few times the free-fall time. Only observations can establish the original M/Φ in clouds; it is
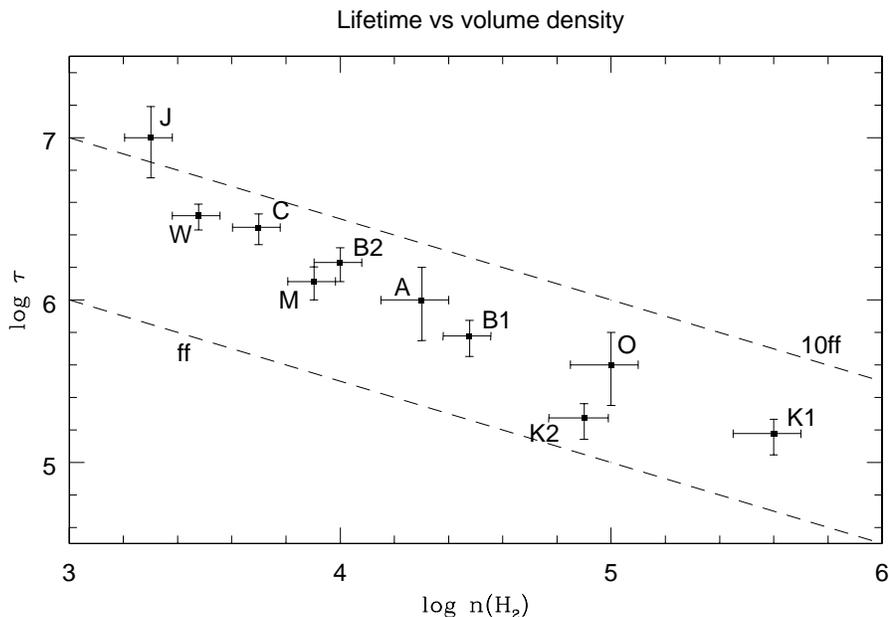
Fig. 2.— A 'JWT plot' (after *Jessop and Ward-Thompson*, 2000) – plot of inferred starless core lifetime against mean volume density (see also: *J. Kirk et al.*, 2005). The dashed lines correspond to models discussed in the text. The symbols refer to literature data as follows: J – *Jessop and Ward-Thompson* (2000); W – *Wood et al.* (1994); C – *Clemens and Barvainis* (1988); B1, B2 – *Bourke et al.* (1995a, 1995b); M – *Myers et al.* (1983); A – *Aikawa et al.* (2005); *Kandori et al.* (2005); O – *Onishi et al.* (2002); K1, K2 – *J. Kirk et al.* (2005).

a free parameter in the theory.

Magnetic fields may also play another crucial role in star formation – transferring angular momentum outward from collapsing, rotating cores, resolving the angular momentum problem and allowing collapse to protostellar densities (*Mouschovias*, 1991). Although supersonic motions are allowed in this paradigm, they do not dominate.

This picture has been challenged by interpretations of observations of the ratio of numbers of starless cores to cores with protostars and young stars that suggest that molecular clouds are short-lived compared with the ambipolar diffusion timescale, and that star formation takes place on a cloud-crossing time (e.g., *Elmegreen*, 2000; *Hartmann et al.*, 2001).

This alternative paradigm is that molecular clouds are intermittent phenomena in an interstellar medium dominated by compressible turbulence (e.g., *MacLow and Klessen*, 2004). Turbulent flows form density enhancements that may or may not be self-gravitating. If self-gravitating, they may be supported against collapse for a short time by the turbulent energy. However, the supersonic turbulence will decay on a short (free-fall) timescale (e.g., *MacLow et al.*, 1998), and collapse will ensue. This would mean that molecular clouds were transient objects, forming and either dissolving quickly or rapidly collapsing to form stars.

One way to distinguish between the theories is to determine the lifetimes of the large-scale molecular clouds. *Hartmann et al.* (2001) argue for short lifetimes, whereas *Tassis and Mouschovias* (2004) and *Mouschovias et al.* (2006) suggest that all available observational data are consistent with lifetimes of molecular clouds as a whole being $\sim 10^7$ yr (see also *Goldsmith and Li*, 2005). Another way is to determine the lifetimes of individual cloud cores. We attempt to do this in the next section. The role of magnetic fields can be assessed by measuring the M/Φ values in cores. We discuss the current data on this in Section 4.

3. OBSERVED CORE LIFETIMES

It was shown in the previous section that it is of vital importance to estimate observationally the timescale of cores with various densities if we are to distinguish between the different model pictures. The numbers of cores detected can be used to determine typical statistical timescales for particular evolutionary stages. This method was first used by *Beichman et al.* (1986), who extrapolated from the typical T Tauri star lifetime and estimated the starless core lifetime to be roughly a few times 10^6 years.

This estimate was subsequently refined by *Lee and Myers* (1999), using an optically-selected sample, to $\sim$0.3–1.6 $\times 10^6$ years for a mean density of $\sim$6–8 $\times 10^3$ cm^{-3}. This age is based upon an estimated range in lifetimes for Class I sources of $\sim$1–5 $\times 10^5$ years. Within this range the best estimate for the Class I lifetime is $\sim$2 $\pm$ 1 $\times 10^5$ years (e.g., *Greene et al.*, 1994; *Kenyon and Hartmann*, 1995). This corresponds to a starless core lifetime of $\sim$6 $\pm$ 3 $\times 10^5$ years.

Towards some molecular cloud complexes optical selection can miss deeply embedded cores in the complex. In these cases, observations in the mm/submm regime are the

best way to observe cores and to carry out the statistical study. For example, *Onishi et al.* (1998, 2002) estimated the time-scale of cores with a density of $\sim 10^5$ cm^{-3} to be $\sim 4 \times 10^5$ years, based on a large-scale molecular line study of cores in Taurus.

J. Kirk et al. (2005) carried out a similar exercise using submm continuum observations of dust in molecular cloud cores. They found a timescale for pre-stellar cores of $\sim 3 \times 10^5$ years with a minimum central density of $\sim 5 \times 10^4$ cm^{-3}. At this density the free-fall time is $\sim 10^5$ years. They made a similar calculation for the cores they classified as 'bright', and derived a time-scale of $\sim 1.5 \times 10^5$ years for cores with a minimum central volume density of $\sim 2 \times 10^5$ cm^{-3}. At this density the free-fall timescale is $\sim 7 \times 10^4$ years.

Kandori et al. (2005) derived detailed radial column density profiles for Bok globules and, by comparison with the theoretical calculations of *Aikawa et al.* (2005), estimated their timescale to be $\sim 10^6$ years for a density of $\sim 2 \times 10^4$ cm^{-3}. A number of other chemical models have been used to carry out a similar exercise in estimating the 'chemical age' of cores (see previous chapter by *Di Francesco et al.*). In many cases this leads to values much longer than a free-fall time.

A similar comparison to that discussed in this section was carried out for a number of different data-sets in the literature by *Jessop and Ward-Thompson* (2000), who plotted the calculated statistical lifetime against the mean volume density of each sample of cores. We reproduce those data here in Figure 2, along with other, more recent data. For example, we include the 'bright' and 'intermediate' cores from *J. Kirk et al.* (2005) – labelled K1 and K2 respectively.

We also plot on Figure 2 some of the model predictions discussed above (following *J. Kirk et al.* 2005). The lower dashed line is the free-fall time, relevant to models such as the highly magnetically supercritical models and the highly dynamic, turbulent models (e.g., *Vazquez-Semadeni et al.*, 2005). The upper dashed line is the power-law formulation of *Mouschovias* (1991) discussed in Section 2 above, for a quasi-static, magnetically subcritical core evolving on the ambipolar diffusion timescale at ten times the free-fall time (*Nakano*, 1998).

In summary, almost all of the literature estimates lie between the two dashed lines on Figure 2. All of the observed timescales are longer than the free-fall time by a factor of ~ 2–5 in the density range of 10^4–10^5 cm^{-3}. Hence we see quite clearly that prestellar and starless cores cannot generally all be in free-fall collapse. Their timescales also appear to be too short for them all to be in a highly magnetically subcritical state. They are all roughly consistent both with mildly subcritical magnetised cores and with models invoking low levels of turbulent support. Hence we must look to observations of magnetic fields to help differentiate between models. In the next section we summarise some of the key observations of magnetic fields.

4. OBSERVATIONS OF MAGNETIC FIELDS

Given that the relative importance of the magnetic field is a key way in which to choose between models, one must try to determine observationally the role of magnetic fields in the star formation process.

Many observations of magnetic fields in regions of low-mass star formation have attempted to test the various paradigms. The observations have utilized the Zeeman effect, mainly in the 18-cm lines of OH (e.g., *Crutcher et al.*, 1993; *Crutcher and Troland*, 2000), and linearly polarized emission of dust at submillimetre wavelengths (e.g., *Ward-Thompson et al.*, 2000; *Matthews et al.*, 2001; *Crutcher et al.*, 2004; *J. Kirk et al.*, 2006).

Unfortunately, the observations are difficult and the results remain somewhat sparse (see, e.g., *Crutcher*, 1999; *Heiles and Crutcher*, 2005). One of the best-studied prestellar cores is L1544, a relatively isolated core in Taurus that has been studied by single-dish (*Tafalla et al.*, 1998) and interferometer spectroscopy (*Williams et al.*, 1999). These studies have suggested that L1544 is contracting.

Information on the magnetic field in L1544 includes OH Zeeman observations with the Arecibo telescope (*Crutcher and Troland*, 2000) and dust polarization mapping with the JCMT SCUBA polarimeter (*Ward-Thompson et al.*, 2000). This cloud is therefore a good example of observational results in low-mass star formation regions.

Figure 3 shows the Arecibo OH Zeeman spectra, which imply a line-of-sight (los) magnetic field strength of $B_{los} = +10.8 \pm 1.7 \, \mu G$, with column density $N(H_2) \approx 4.8 \times 10^{21}$ cm^{-2}, mean radius $\overline{r}(OH) \approx 0.08$ pc, and volume density $n(H_2) \approx 1 \times 10^4$ cm^{-3}. Because all three components of the magnetic field vector are not generally observed, and because the inferred column densities are not generally along the direction of the magnetic field vector, the directly observed M/Φ is typically an overestimate of the true value. A statistical correction for this is possible (see *Heiles and Crutcher*, 2005). For a large randomly oriented sample, the observed M/Φ average should be divided by 3 to obtain the statistically correct result. This correction may be applied to each cloud individually, but it must be kept in mind that this correction is only strictly valid for a large sample of measurements. The directly observed M/Φ for L1544 is ≈ 3.4. *Crutcher and Troland* (2000) corrected this value statistically for geometrical bias, finding $M/\Phi \approx 1.1$, or roughly critical.

Figure 3 also shows the SCUBA dust intensity and polarized intensity map of L183 (*Crutcher et al.*, 2004). *Ward-Thompson et al.* (2000) had previously mapped L183 and two other prestellar cores – L1544 and L43. *Crutcher et al.* (2004) used the Chandrasekhar-Fermi (CF) method (*Chandrasekhar and Fermi*, 1953) to measure the magnetic field strengths and hence the relative criticality of all three cores.

In Figure 3 the polarisation half vectors have been rotated by 90° to indicate the plane-of-sky (pos) magnetic field direction (a half vector is a vector with a 180° bi-directional ambiguity, such as we have here). The field is
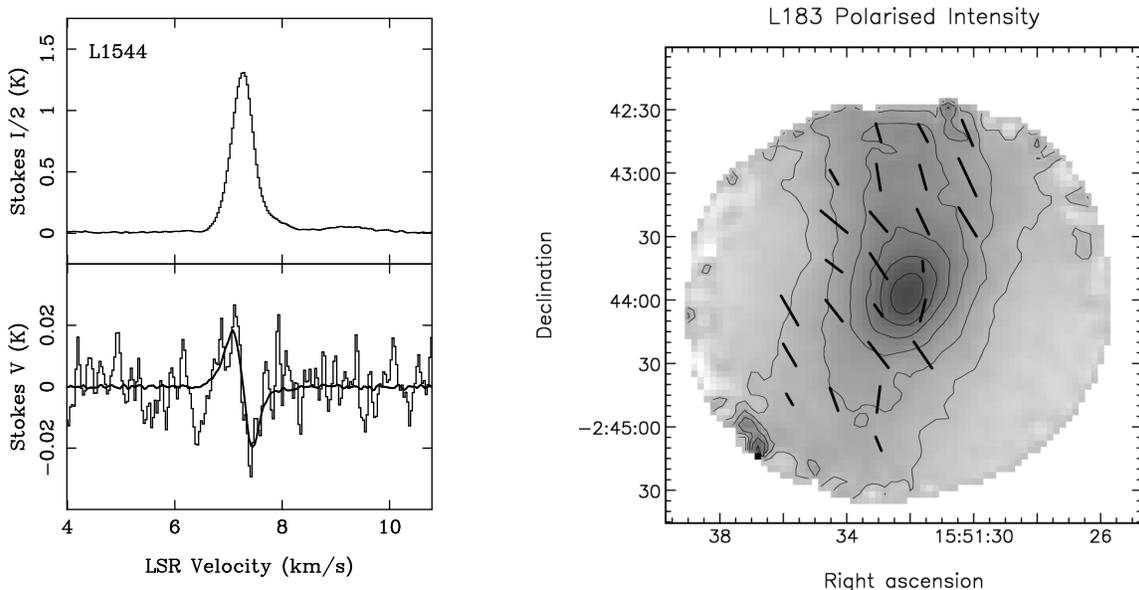
Fig. 3.— Plot of Arecibo OH Zeeman spectra (left) in the prestellar core L1544, from *Crutcher and Troland* (2000), and SCUBA submillimetre dust intensity and polarised intensity data of prestellar core L183 (right), from *Crutcher et al.* (2004). The polarised intensity half vectors have been rotated by $90°$ to show the plane-of-sky magnetic field direction.

seen to be fairly uniform in direction in L183, as it was in L1544 and L43, with a position angle dispersion $\delta\phi \approx 14°$, but the direction of the field in the plane of the sky is at an angle of $34° \pm 7°$ to the minor axis.

This difference between the magnetic field direction and the minor axis of the core is in conflict with symmetric models that rely only on thermal and static magnetic pressure to balance gravity, since the minor axis projected onto the sky should lie along B_{pos}. However, projection effects can produce the observed position angle difference if the core has a more complicated shape, such as a triaxial geometry (*Basu*, 2000). The initial conditions of cloud formation and turbulence may produce the more complicated shapes (*Gammie et al.*, 2003).

The physical parameters of the L1544 prestellar core inferred from the SCUBA data (*Crutcher et al.*, 2004) are: $\overline{r}(dust) \approx 0.021$ pc, $N(H_2) \approx 4.2 \times 10^{22}$ cm^{-2}, $n(H_2) \approx 4.9 \times 10^5$ cm^{-3}, and total mass $M \approx 1.3 \, M_\odot$. With the velocity dispersion $\Delta V_{NT} \approx 0.28$ km s^{-1}, as measured from N_2H^+ data (*Caselli et al.*, 2002), the CF method yielded $B_{pos} \approx 140 \, \mu G$. Then $M/\Phi \approx 2.3$, (*Crutcher et al.*, 2004) and the statistically corrected value is then $M/\Phi \approx 0.8$. Hence L1544 is approximately critical or mildly supercritical.

The M/Φs for L1544 found from the OH Zeeman and the dust polarization techniques are essentially in agreement, but very different regions are sampled by the two methods. The region sampled by OH has 4 times the radius, 0.1 times the column density, and 0.02 times the volume density of the region sampled by the dust emission. Therefore, the data probe separately the envelope and the core regions of the cloud.

We have argued that the two M/Φ values are consistent to within the errors, but if the difference between them were real, then M/Φ decreases from envelope to core, the opposite of the ambipolar diffusion prediction. However, the Zeeman effect measures B_{los} and dust emission measures B_{pos}, and we do not know the inclination of **B** to the line of sight. Direct measurement of an increase in M/Φ from envelope to core would strongly support the ambipolar diffusion model. However, present data do not allow one to do this.

Other prestellar cores have recently been mapped in submm polarisation. *J. Kirk et al.* (2006) mapped two cores, L1498 and L1517B. They measured the magnetic field strength by the CF method and estimated both the (non-magnetic) virial mass and the magnetic critical mass. In both cases they found the prestellar cores to be supercritical by a factor of ∼2–3. For comparison the three cores of *Crutcher et al.* (2004) were also seen to be mildly supercritical, as predicted by the ambipolar diffusion model.

However, when *J. Kirk et al.* (2006) calculated the magnetic virial mass (i.e. including the effects of both magnetic fields and turbulent line-widths) they found the cores to be roughly virialised, with the magnetic field providing roughly half of the support (as was the case for the three cores studied by *Crutcher et al.* 2004).

Hence we see that for the five prestellar cores whose magnetic fields have been studied in detail, both turbulence and magnetic fields are seen to be playing a roughly equal role in the support against gravitational collapse, and thus in the evolution of the cores (*J. Kirk et al.*, 2006). These cores are all relatively isolated and moderately quiescent cases, and all give a similar result. Thus we may perhaps conclude
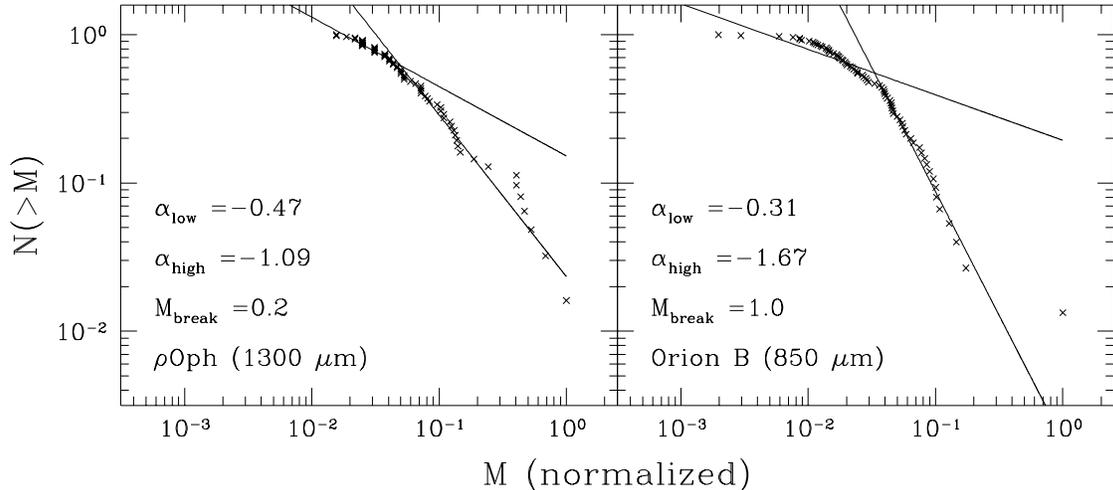
Fig. 4.— Plot of normalised core mass function for the ρ Oph and Orion molecular clouds (adapted from *Reid*, 2005; based on original data from *Motte et al.*, 1998; and *Johnstone et al.*, 2000). The two slopes and break-point mass of double power law fits are given in each panel. The break-point masses are quoted in $M_\odot$. Note the similarity to the stellar initial mass function (e.g., *Kroupa*, 2002).

that for isolated star formation in fairly quiescent molecular clouds, one must consider the influences of mildly turbulent motions and magnetic fields together. Finally, we note that similar submillimetre dust polarization results have been obtained for a number of Class 0 protostellar cores (e.g., *Matthews and Wilson*, 2002; *Wolf et al.*, 2003).

5. CORE MASS FUNCTION

The last seven years since PPIV have seen some progress in measuring the mass function of cold cores in molecular clouds with a wide range of intrinsic mass scales. This progress has been made possible by the availability of new, sensitive cameras at millimetre and submillimetre wavelengths (e.g., *Kreysa et al.*, 1999; *Holland et al.*, 1999).

Wide-area millimetre continuum mapping of the Ophiuchus molecular cloud (*Motte et al.*, 1998) first revealed a core mass function that bears a striking similarity to the stellar initial mass function (IMF – e.g., *Kroupa*, 2002; *Chabrier*, 2003). This was subsequently confirmed by others – e.g., in Serpens (*Testi and Sargent*, 1998), ρ Oph (*Johnstone et al.*, 2000; *Reid and Wilson*, 2006; *Stanke et al.*, 2006), and Orion (*Motte et al.* 2001; *Johnstone et al.*, 2001, 2006; *Nutter*, 2004; *Reid and Wilson*, 2006). Figure 4 shows the core mass functions for ρ Oph and Orion (*Reid and Wilson*, 2006), based on the original results of *Motte et al.* (1998) and *Johnstone et al.* (2000).

In all of these regions the slope of the cumulative core mass function above 0.5–1 $M_\odot$ is −1.0 to −1.5 (see Figure 4), in good agreement with the high-mass slope of −1.35 for the stellar IMF (*Salpeter*, 1955). The core mass function is observed to have a shallower slope at smaller masses, although it has been questioned as to whether the change in slope at lower masses is an intrinsic property of the clump mass function or is caused by some kind of incompleteness in the observations (e.g., *Johnstone et al.*, 2000, 2001).

In addition, the peak of the core mass function in each of these cluster-forming regions lies in the range of 0.2–1 $M_\odot$ (in $dN/d\log M$ format), only slightly larger than the peaks of the mass functions of ~ 0.08 $M_\odot$ for single stars and ~ 0.2 $M_\odot$ for multiple systems (*Chabrier*, 2003). In short, both the shape and the intrinsic scale of the core mass function in these regions appear to be well-matched to the observed properties of the stellar IMF.

Some similar work on more distant, higher mass regions has also been carried out (e.g., *Tothill et al.*, 2002; *Motte et al.*, 2003; *Mookerjea et al.*, 2004; *Beuther and Schilke*, 2004; *Reid and Wilson*, 2005, 2006), although this is strictly beyond the scope of this chapter on low-mass cores. In addition, these studies suffer from problems such as: a cluster of low-mass cores can appear, in these more distant regions, to merge into a single higher-mass core; any incompleteness in the mass function will set in at relatively higher masses; and most of these studies make no distinction between starless cores and those with protostars.

It has been suggested that the fact that the shape of the core mass function does not appear to vary from region to region even as its intrinsic scale is changing, appears to be consistent with the core mass function being determined primarily by turbulent fragmentation (e.g., *Reid*, 2005). However, this result is subject to the caveats mentioned above. Nonetheless, numerical simulations by several groups have shown that turbulent fragmentation can produce clump mass functions whose shape does not de-
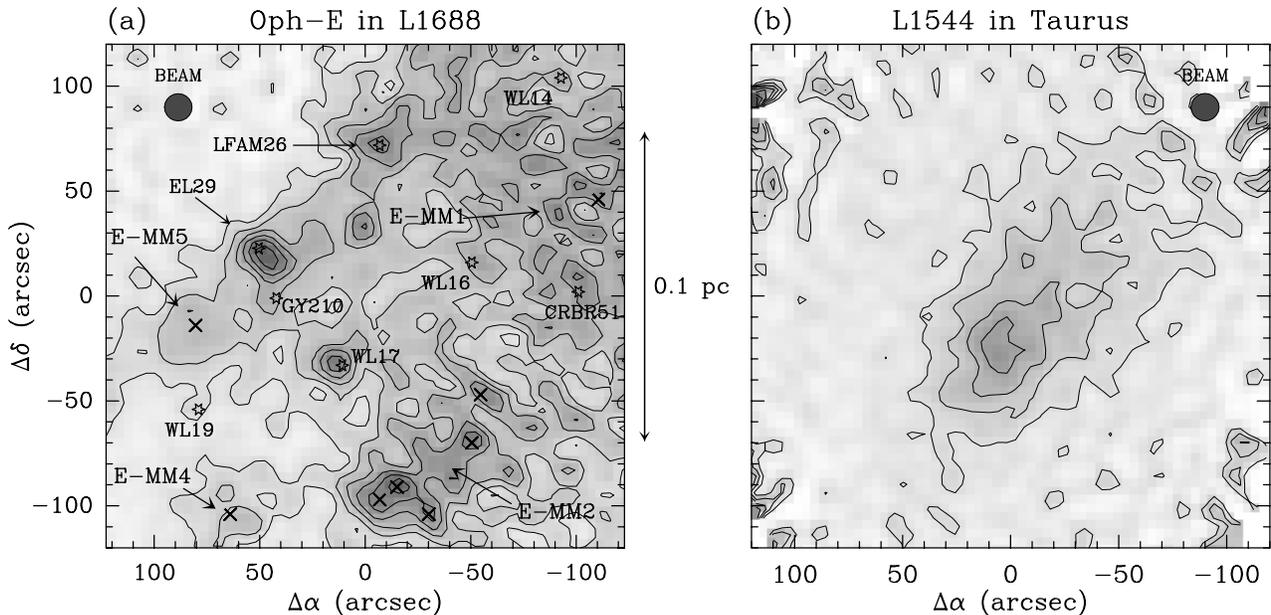
Fig. 5.— Millimetre dust continuum images of ρ Oph-E (left) and Taurus (right) taken at the same resolution with the IRAM 30-m telescope (from *Motte et al.*, 1998 and *Ward-Thompson et al.*, 1999 respectively). Note how the cluster-forming ρ Oph core shows far more substructure than the more isolated Taurus pre-stellar core at the same linear scale. In the left-hand image the crosses mark starless cores and the stars mark protostellar objects.

pend strongly on the intrinsic mass scale of the region (*Klessen et al.*, 1998; *Klessen and Burkert*, 2000; *Klessen*, 2001a; *Padoan and Nordlund*, 2002; *Gammie et al.*, 2003; *Tilley and Pudritz*; 2004).

6. CLUSTER-FORMING VS ISOLATED CORES

The environment in which a core forms is crucial to its subsequent evolution. This has been known for some time. The sequential model of star formation (*Lada*, 1987) predicts that where young stars have already formed, their combined effects will cause further star formation in the remainder of the molecular cloud. This was seen, for example, in the ρ Oph molecular cloud, where *Loren* (1989) hypothesised that the upper Sco OB association was triggering star formation in L1688. Further evidence in support of this hypothesis was provided by a comparison of the relative star-formation activity in L1688 and L1689 (*Nutter et al.*, 2006), wherein these two adjacent clouds were seen to have very different levels of star formation due to L1689 being further from the OB association.

Furthermore, the dense cores that are observed on a ~ 0.1 pc scale in nearby cluster-forming clouds using classical high-density tracers, such as NH_3, N_2H^+, $H^{13}CO^+$, DCO^+, $C^{18}O$, and dust continuum emission, tend to have higher masses and column densities than isolated prestellar cores (e.g., *Jijina et al.*, 1999). Figure 5 shows a comparison between the Taurus and central Ophiuchus star-forming regions. It can be seen that the region occupied by a typical

single prestellar core in Taurus plays host to a small cluster in Ophiuchus. Moreover, the level of cluster-forming activity in a core clearly correlates with core mass and column density (e.g., *Aoyama et al.*, 2001).

High column-density, cluster-forming cores are typically fragmented and show a great deal of substructure (see Figure 5a). Submillimetre dust continuum mapping of the ρ Oph, Serpens, and Orion B cluster-forming cores has revealed a wealth of compact starless and pre-stellar cores (e.g., *Motte et al.*, 1998, 2001; *Johnstone et al.*, 2000, 2001; *Kaas et al.*, 2004; *Testi and Sargent*, 1998), which appear to be the direct precursors of individual stars or systems. In particular, their mass distribution is remarkably similar to the stellar IMF (see Section 5 above).

These prestellar cores in clusters are denser ($< n > \gtrsim 10^6$–10^7 cm^{-3}), more compact (diameter $D \sim 0.02$–0.03 pc), and more closely spaced ($L \sim 0.03$ pc) than isolated prestellar cores, such as those seen in Taurus, which typically have $< n > \gtrsim 10^5$ cm^{-3}, $D \sim 0.1$ pc, and $L \sim 0.25$ pc. (e.g., *Onishi et al.*, 2002; previous chapter by *Di Francesco et al.*).

We define the local star-forming efficiency (SFE$_{pre}$) associated with a prestellar core as:

$$SFE_{pre} = \frac{M_*}{M_{pre}}$$

where M_{pre} is the initial mass of a prestellar core that forms a star of mass M_*. We find that the star formation efficiency within prestellar cores in cluster-forming regions is high.
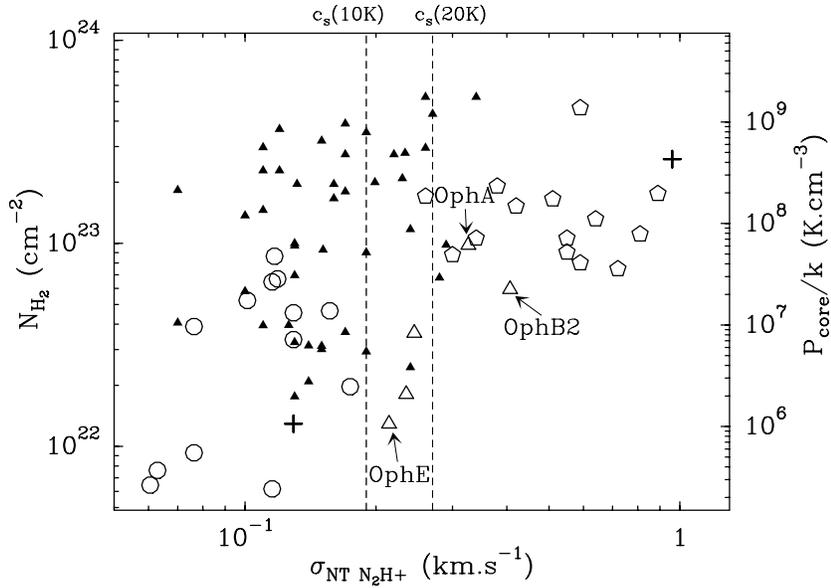
Fig. 6.— Plot of column density against non-thermal velocity dispersion in low-mass dense cores (following *André et al.*, 2006). The two vertical dashed lines represent the sound speeds for 10K and 20K gas respectively. The open circles represent the isolated prestellar cores in Taurus. The large, open triangles are the cluster-forming cores in ρ Oph. The small, filled triangles are the prestellar cores in ρ Oph (*Motte et al.*, 1998; *André et al.*, 2006). The large, open pentagons are the cluster-forming cores in NGC2264D (*Peretto et al.*, 2006). The two crosses are two equilibrium models representative of quasi-static scenarios for low-mass (lower left) and high-mass (upper right) star formation (cf. *Shu et al.*, 1987; and *McKee and Tan*, 2003, respectively). Note the broad trend seen in the open symbols, and that cluster-forming cores lie on the right-hand (supersonic) side of the figure, while prestellar cores lie on the left-hand (subsonic) side. Note also that most of the prestellar cores in the cluster-forming region of ρ Oph lie above the 'sequence' observed in the open polygons, at up to an order of magnitude higher densities than isolated prestellar cores.

Most of their initial mass at the onset of collapse appears to end up in a star or stellar system: $SFE_{pre} \geq 50\%$ (cf. *Motte et al.*, 1998; *Bontemps et al.*, 2001). This contrasts with the lower ($\sim 15\%$) local star formation efficiency associated with the isolated prestellar cores in Taurus (*Onishi et al.*, 2002).

Interestingly, extensive searches for cores in the Ophiuchus and Pipe Nebula complexes (e.g., *Onishi et al.*, 1999; *Tachihara et al.*, 2000; *Johnstone et al.*, 2004; *Nutter et al.*, 2006) suggest that cluster-forming cores and prestellar cores can only form in a very small fraction of the volume of any given molecular cloud complex, typically at a compressed extremity.

Recent analysis of the physical conditions within cluster-forming molecular clouds has revealed an apparent extinction threshold criterion. *Johnstone et al.* (2004) noted that in Ophiuchus almost all cores were located in high extinction regions ($A_V > 10$), despite the fact that most of the cloud mass was found at much lower extinctions (cf. Figure 1).

Analysis of the Perseus cloud (*H. Kirk*, 2005; *H. Kirk et al.*, 2006; *Enoch et al.*, 2006) reveals a similar extinction threshold, although at a somewhat lower value ($A_V > 5$). These results are in agreement with the analysis of Taurus using $C^{18}O$ by *Onishi et al.* (1998), who found that only regions with column densities above N(H$_2$)= 8×10^{21} cm^{-2} ($A_v \sim 8$) contained IRAS sources, indicating that high column density is necessary for star formation.

These observations are in fact consistent with the idea that magnetic fields play an important role in supporting molecular clouds (*McKee*, 1989). The outer region of the cloud is maintained at a higher fractional ionization level by ultraviolet photons from the interstellar radiation field. However, the ultraviolet photons cannot penetrate deep into the cloud due to extinction.

The ionization fraction thus drops in the inner region, shortening the ambipolar diffusion timescale. According to this scenario, one expects small-scale structure and star formation to proceed only in the inner, denser regions of the cloud. McKee estimates the column density depth required for sufficient ultraviolet attenuation to be in the region of $A_V \sim 4 - 8$.

Column density and linewidth are among the key parameters for a core in determining its evolution. Figure 6 plots the column density N(H$_2$) versus the non-thermal velocity dispersion σ_{NT}, measured in the N$_2$H$^+$ line, for a large number of cores. The open circles are isolated prestellar cores. The open triangles and pentagons are cluster-forming cores. The filled triangles are prestellar cores in cluster-forming regions.

It is seen that the cluster-forming cores of, for example, Ophiuchus, Serpens, Perseus and Orion have linewidths dominated by non-thermal motions (e.g., *Jijina et al.*, 1999; *Aso et al.*, 2000). They are significantly more turbulent than the more isolated prestellar cores of Taurus, whose linewidths are dominated by thermal motions (e.g., *Tatematsu et al.*, 2004; *Benson and Myers*, 1989). In plotting

Figure 6 we have removed the thermal velocities and plot only the non-thermal velocity dispersions.

However, the more compact (~ 0.03 pc) prestellar cores observed within cluster-forming regions are characterized by fairly narrow N$_2$H$^+$(1-0) linewidths ($\Delta V_{FWHM} \lesssim 0.5$ km s^{-1}), more reminiscent of the isolated prestellar cores of Taurus (*Belloche et al.*, 2001). This indicates subsonic or at most transonic levels of internal turbulence and suggests that, even in cluster-forming clouds, the initial conditions for individual protostellar collapse are relatively free of supersonic turbulence. It can be seen from Figure 6 that the nonthermal velocity dispersion, measured toward the prestellar cores of the ρ Oph cluster is only a fraction (typically 0.5–1) of the isothermal sound speed (*Belloche et al.*, 2001; *André et al.*, 2006).

The narrow N$_2$H$^+$ line widths measured for the prestellar cores in these clusters imply virial masses which generally agree well with the mass estimates derived from the dust continuum. This confirms that most of the starless cores identified in the submm dust continuum are self-gravitating and very likely prestellar in nature.

Furthermore, Figure 6 appears to show that the prestellar cores in a cluster-forming region such as ρ Oph (filled triangles) largely occupy a different parameter space from the isolated prestellar cores of Taurus (open circles). This tends to imply a different formation mechanism for prestellar cores in isolated and clustered regions, with the latter forming by fragmentation of higher-mass, more turbulent, cluster-forming cores (cf. *Myers*, 1998). For this reason (following *Motte et al.*, 2001), we suggest that prestellar cores in clustered regions could perhaps be called prestellar condensations to indicate this difference.

In addition, there appears to be a broad trend of increasing velocity dispersion with increasing column density from isolated prestellar cores to cluster-forming cores (cf. *Larson*, 1981). This perhaps reflects the fact that all of these cores are self-gravitating, hence characterized by virial mass ratios close to unity. Higher density cores form in clustered regions, where the ambient pressure is higher, and subsequently fragment before forming stars.

One of the clear signposts of star formation is direct detection of infall. Detection of blue infall profiles (see previous chapter by *Di Francesco et al.*) in optically thick line tracers such as HCO$^+$(3–2) toward a number of starless cores in cluster-forming regions (e.g., OphE-MM2 in ρ Oph – *Belloche et al.*, 2001) suggests that some of them are in fact already collapsing and on the verge of forming protostars.

Prestellar cores in low-mass proto-clusters also appear to be characterized by small core-core relative motions (e.g., *Walsh et al.*, 2004). For instance, based on the observed distribution of N$_2$H$^+$(1–0) line-of-sight velocities, a global, one-dimensional velocity dispersion σ_{1D} of < 0.4 km s^{-1} was found for the cores of the ρ Oph cluster (*Belloche et al.*, 2001; *André et al.*, 2006).
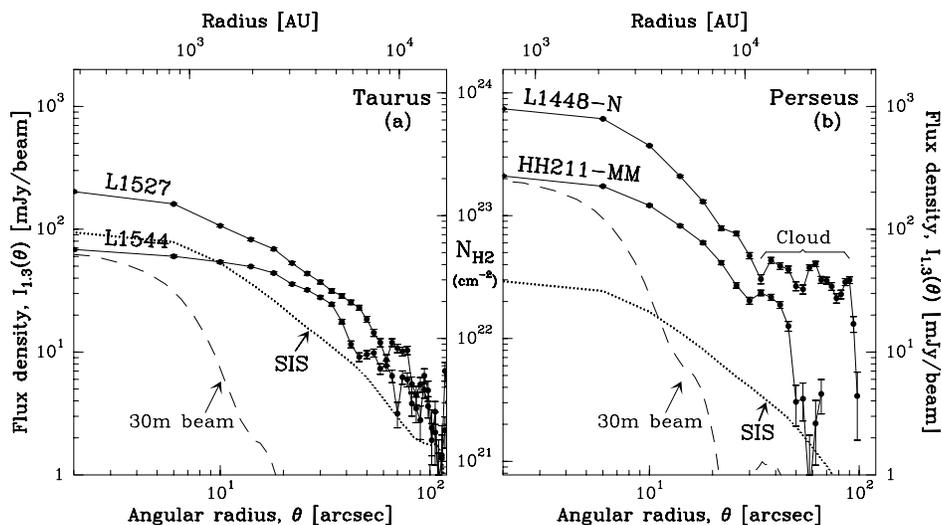
Fig. 7.— Radial density profiles in Taurus (left) and Perseus (right) – from *Motte and André* 2001. In Taurus we show a prestellar core, L1544, and a Class 0 protostar, L1527. In Perseus we show two Class 0 protostars, L1448-N and HH211-MM. The dotted line marked SIS shows the initial conditions for spontaneous collapse (e.g., *Shu et al.*, 1987) convolved with the beam (dashed line). Note that the prestellar core has a flatter profile than the protostellar cores and that the column densities in Perseus are an order of magnitude higher than both the model and the Taurus cores.

7. FROM CORES TO PROTOSTARS

Most of the starless cores and all of the prestellar cores that we have been discussing are expected to evolve into Class 0 protostars (*André et al.*, 1993, 2000) and subsequently into Class I protostars (*Lada*, 1987; *Wilking et al.*, 1989). Therefore, another approach to constraining the initial conditions for protostellar collapse consists of studying the structure of young Class 0 protostars. These objects are observed early enough after point mass formation that they still retain some memory of their initial conditions (cf. *André et al.*, 2000).

By comparing the properties of prestellar cores with those of Class 0 cores, we can hope to bracket the physical conditions at point mass formation. Furthermore, since Class 0 objects have already begun to form stars at their centres, we can be sure that they are participating in the star-formation process (which is not certain for all starless cores). In fact, in some cases it is difficult to differentiate between the most centrally-condensed prestellar cores and the youngest Class 0 protostars. Examples of low-luminosity, very young Class 0 protostars that look like prestellar cores include L1014 (*Young et al.*, 2004; *Bourke et al.*, 2005) and MC27/L1521F (*Onishi et al.*, 1999) – see also previous chapter by *Di Francesco et al.*

When discussing the density and velocity structure of Class 0 envelopes, we here again contrast isolated and clustered objects. In terms of their density profiles, protostel-

lar envelopes are found to be more strongly centrally condensed than prestellar cores, and do not exhibit any marked inner flattening in their radial column density profiles (see Figure 7), unlike prestellar cores (*J. Kirk et al.*, 2005).

In regions of isolated star formation such as Taurus, protostellar envelopes have radial density gradients consistent with $\rho(r) \propto r^{-p}$ with $p \sim 1.5$–2 over ~ 10000–15000 AU in radius (e.g., *Chandler and Richer*, 2000; *Hogerheijde and Sandell*, 2000; *Shirley et al.*, 2000, 2003; *Motte and André*, 2001). Furthermore, the absolute level of the density distributions observed towards Taurus Class 0 sources is roughly consistent with the predictions of spontaneous collapse models (see Figure 7) starting from quasi-equilibrium, thermally-dominated prestellar cores (e.g., *Hennebelle et al.*, 2003).

By contrast, in cluster-forming regions such as Serpens, Perseus, or ρ Oph, Class 0 envelopes are clearly not scale-free. They merge either with other cores or other protostellar envelopes, or the ambient cloud, at a finite radius $R_{out} \lesssim 5\,000$ AU (*Motte et al.*, 1998; *Looney et al.*, 2003). They are also typically an order of magnitude more dense than models of the spontaneous collapse of isothermal (e.g., Bonnor-Ebert) spheres predict immediately after point mass formation (cf. *Motte and André*, 2001) – see Figure 7.

Turning to velocity profiles, the surrounding environment can play an important role in the mass infall rate, since in a clustered environment this can vary strongly even for protostars with similar final masses (*Klessen*, 2001b).
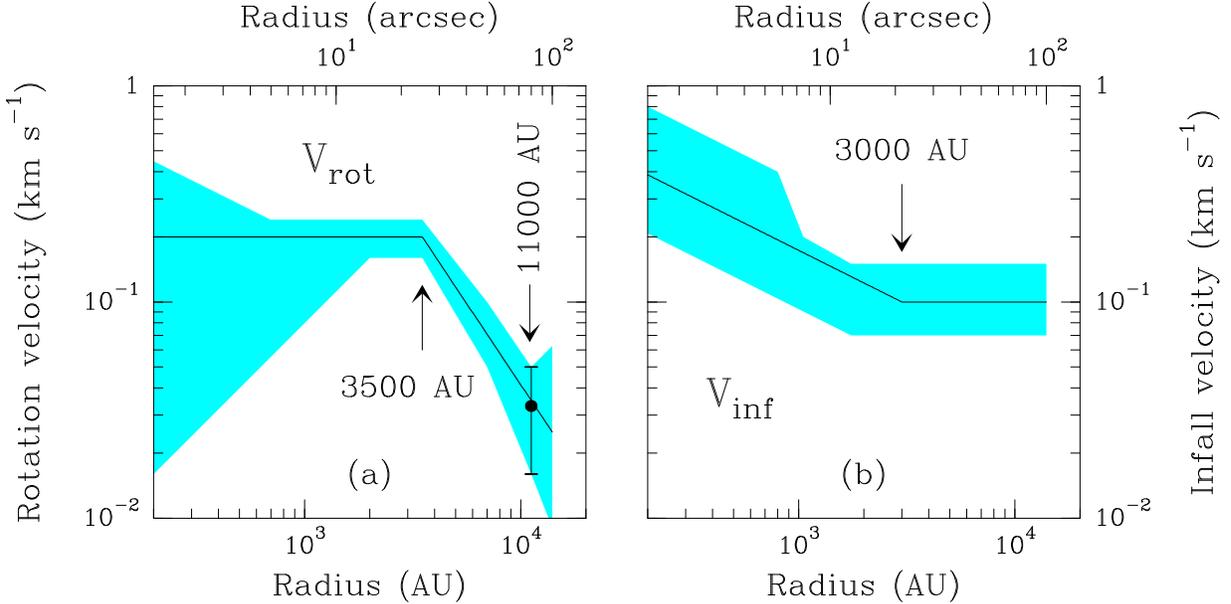
Fig. 8.— Velocity profiles in the Class 0 protostellar core IRAM 04191. Rotational velocity (left) and infall velocity (right) are plotted as a function of radius (from *Belloche et al.*, 2002). The inner part of the envelope is rapidly collapsing and rotating, while the outer part undergoes only moderate infall and slower riotation.

Models suggest that the mass infall rate may be a strongly varying function of time, with a peak infall rate occurring in the Class 0 stage (e.g., *Henriksen et al.*, 1997; *Whitworth and Ward-Thompson*, 2001; *Schmeja and Klessen*, 2004). The mean mass infall rate is also predicted to decrease as the Mach number of the turbulence increases (*Schmeja and Klessen*, 2004). In addition, the relative importance of turbulent and gravitational energy can change the number of binary systems that are formed as well as their properties, such as semi-major axis and mass ratio (*Goodwin et al.*, 2004).

There have been few detailed studies of velocity profiles, but one example of an isolated Class 0 object is IRAM 04191 in Taurus (see Figure 8 and *Belloche et al.*, 2002). In this case, the inner part of the envelope ($r \lesssim 2000 - 4000$ AU) is rapidly collapsing and rotating, while the outer part ($4000 \lesssim r \lesssim 11000$ AU) undergoes only moderate infall and slower rotation. This dramatic drop in rotational velocity beyond $r \sim 4000$ AU, combined with the flat infall velocity profile, suggests that angular momentum is conserved in the collapsing inner envelope but efficiently dissipated, perhaps due to magnetic braking, in the slowly contracting outer envelope.

The mass infall rate of IRAM 04191 is estimated to be $\dot{M}_{inf} \sim 3 \times 10^{-6}$ $M_\odot$ yr^{-1}, which is $\sim 2 - 3$ times the canonical a_s^3/G value often used (where $a_s \sim 0.15 - 0.2$ km s^{-1} is the isothermal sound speed). Similar $\dot{M}_{inf}$ values have been reported for several other bona-fide

Class 0 and Class I protostars in Taurus (e.g., *Ohashi*, 1999; *Hirano et al.*, 2002).

A very different example in a clustered region is IRAS 4A in the NGC 1333 protocluster. *Di Francesco et al.* (2001) observed inverse P-Cygni profiles towards IRAS 4A, from which they derived a very large mass infall rate $\sim 1.1 \times 10^{-4}$ $M_\odot$ yr^{-1} at $r \sim 2000$ AU. A similar infall rate was independently found by *Maret et al.* (2002).

This value of $\dot{M}_{inf}$ corresponds to more than ~ 15 times the canonical a_{eff}^3/G value (where $a_{eff} \lesssim 0.3$ km s^{-1} is the effective sound speed). This high infall rate results both from a very dense envelope and a large, supersonic infall velocity – ~ 0.68 km s^{-1} at ~ 2000 AU (*Di Francesco et al.*, 2001).

Other examples of Class 0 protostars in cluster-forming regions with quantitative estimates of the mass infall rate include NGC 1333-IRAS2, Serpens-SMM4, and IRAS 16293. In all of these objects, high $\dot{M}_{inf}$ values $\gtrsim 3 \times 10^{-5}$ $M_\odot$ yr^{-1} are found (e.g., *Ceccarelli et al.*, 2000; *Ward-Thompson and Buckley*, 2001).

The velocity structures of prestellar cores have also been studied in some cases. The isolated prestellar core L1544 has been seen to have a 'flat' velocity profile over a wide range of radii, with no evidence for velocity increasing towards the centre (*Tafalla et al.*, 1998; *Williams et al.*, 1999). Infall profiles have also been observed in a number of other prestellar cores at large radii (e.g., *Lee et al.*, 1999; *Gregersen and Evans*, 2000) and it seems that a sig-

nificant number may already be contracting (see previous chapter by *Di Francesco et al.*).

The observational constraints summarized above have strong implications for collapse models. First, the extended infall velocity profiles observed in prestellar cores and young Class 0 objects are inconsistent with pure inside-out collapse and in better agreement with isothermal collapse models starting from Bonnor-Ebert spheres (e.g., *Whitworth and Summers*, 1985; *Foster and Chevalier*, 1993), or similar density profiles (e.g., *Whitworth and Ward-Thompson*, 2001).

For isolated cores, the fact that the measured infall velocities are subsonic and that there is indirect evidence of magnetic braking (*Belloche et al.*, 2002 – see above) suggests that the collapse is spontaneous and moderated by magnetic effects in mildly magnetized versions of Bonnor-Ebert cloudlets (cf. *Basu and Mouschovias*, 1994). In Taurus, the measured infall rates seem to rule out models based on competitive accretion (e.g., *Bonnell et al.*, 2001) or gravo-turbulent fragmentation (e.g. *Schmeja and Klessen* 2004) which predict large time and spatial variations of $\dot{M}_{inf}$.

By contrast, in protoclusters such as NGC 1333 or ρ Oph, the large overdensity factors measured in Class 0 envelopes compared to hydrostatic isothermal structures, as well as the supersonic infall velocities and very high infall rates observed in some cases, are inconsistent with self-initiated forms of collapse and require strong external compression.

This point is supported by recent numerical simulations of the collapse of Bonnor-Ebert spheres (*Hennebelle et al.*, 2003, 2004), which show that large overdensity factors, together with supersonic infall velocities, and high infall rates ($\gtrsim 10\,a_s{}^3/G$) are produced near point mass formation when, and only when, the collapse is induced by a strong and rapid increase in external pressure (see also *Motoyama and Yoshida*, 2003).

The high infall rates at the Class 0 stage, as well as the strong decline of $\dot{M}_{inf}$ observed between the Class 0 and the Class I stage in clusters (e.g., *Henriksen et al.*, 1997; *Whitworth and Ward-Thompson*, 2001), can also be reproduced in the context of the turbulent fragmentation picture (cf. *Schmeja and Klessen*, 2004), according to which dense cores form by strong turbulent compression (e.g., *Padoan and Nordlund*, 2002).

8. DISCUSSION AND CONCLUSIONS

We have presented observational results that bear on the evolution of dense low-mass cores in an endeavour to estimate which aspects of the continuum of models discussed in Section 2 above relate to the different environments of star formation that we observe. The formation and evolution of cores is crucial to an understanding of the star formation process, not least because the results presented in Section 5 indicate that the core mass function has a very strong bearing on the stellar IMF. The results summarized in Section 6 help to discriminate between possible theoretical scenarios for the formation and evolution of isolated cores compared to cluster-forming cores.

The narrow linewidths observed in prestellar cores in cluster-forming regions are in qualitative agreement with the picture according to which such cores form by dissipation of internal MHD turbulence (e.g., *Nakano*, 1998 – cf. Figure 6). These cores may correspond to self-gravitating 'kernels', of size comparable to the cutoff wavelength for MHD waves (e.g., *Kulsrud and Pearce*, 1969), that can develop only in turbulent cloud cores (e.g., *Myers*, 1998).

However, at variance with this picture, we see that some cluster-forming cores such as ρ Oph E (*Belloche et al.*, 2001) also exhibit narrow line widths (see Figure 6), similar to those of the prestellar cores within them. This tends to suggest that spontaneous dissipation of internal MHD turbulence may not be the only mechanism responsible for core fragmentation. In an alternative view, the formation of cluster-forming cores may primarily reflect the action of a strong external trigger at the head of elongated, head-tail cloud structures (e.g., *Tachihara et al.*, 2002; *Nutter et al.*, 2006).

A marked increase in external pressure resulting from the propagation of neighbouring stellar winds and/or supernova shells into a cloud can indeed significantly reduce the critical Bonnor-Ebert mass and the corresponding Jeans fragmentation lengthscale (cf. *Nakano*, 1998). It may also trigger protostellar collapse (e.g., *Boss*, 1995) and account for the enhanced infall rates observed at the Class 0 stage in cluster-forming clouds (see Section 7).

Furthermore, the small velocity dispersions measured for the prestellar cores in the ρ Oph cluster, imply a crossing time, $\sim 2 \times 10^6$ yr (*Belloche et al.*, 2001; *André et al.*, 2006), that is larger than the estimated core lifetime ($< 2.5 \times 10^5$ yr – see Section 3). This suggests that typical prestellar cores in clusters do not have time to interact with one another before collapsing to protostars. Taken at face value, this seems inconsistent with models which resort to dynamical interactions to build up a mass spectrum comparable to the IMF (e.g., *Bate et al.*, 2003; *Bonnell et al.*, 2003). Nonetheless these models may still be relevant in higher-mass star-forming regions (cf. *Peretto et al.*, 2006).

Therefore, it appears that the influence of the external environment plays a crucial role in the formation and evolution of low-mass dense cores. An isolated, low-density, quiescent environment will most likely lead to a more quasi-static evolution. A clustered, dense environment in which the external pressure is increased by the action of nearby, newly-formed stars, will probably yield a more dynamic evolutionary scenario.

The fact that most isolated prestellar cores appear to be within a factor of a few of magnetic criticality suggests that the magnetic field is playing an important role and is consistent with the ambipolar diffusion picture (see Section 4). However, whether or not this role is dominant depends on the balance between the field strength and the other environmental factors.

9. FUTURE DEVELOPMENTS

There are many exciting developments in telescopes and instrumentation planned in the next few years that will impact this field. These include new, more sensitive cameras for single-dish telescopes, such as SCUBA-2 on the James Clerk Maxwell Telescope (JCMT) as well as SPIRE and PACS on the Herschel Space Observatory, and new interferometers such as the Combined Array for Research in Millimeter-wave Astronomy (CARMA) and the Atacama Large Millimetre Array (ALMA).

The new submillimetre cameras on JCMT and Herschel will increase our wide-area mapping coverage, so that for example, SCUBA-2 and SPIRE will map almost all star-forming regions within 0.5 kpc. These observations will produce a flux-limited, multi-wavelength snapshot of star formation near the Sun, providing a legacy of images, as well as point-source and extended-source catalogues covering up to 700 square degrees of sky.

On small scales, the Herschel observations will, for the first time, resolve the detailed dust temperature structure of the nearest isolated prestellar cores. On global molecular cloud scales, the large spatial dynamic range of the Herschel images will provide a unique view of the formation of both isolated prestellar cores and cluster-forming cores.

CARMA will bring improved angular resolution (~ 0.13 arcsec) and sensitivity – ~ 25 times better than the Berkeley Illinois Maryland Array (BIMA) – to mm-wave polarization studies of the dust and molecular line emission in dense clouds and lead to routine high-resolution polarization mapping. These instrumental gains will enable Zeeman mapping of the CN J=(1→0) transition and measurement of line-of-sight magnetic field strengths at densities $n(H_2) \sim 10^{5-6}$ cm^{-3} and mapping of dust and CO linearly polarized emission toward both high-mass and low-mass star-formation regions.

The Atacama Large Millimeter Array (ALMA) will have more than an order of magnitude greater sensitivity and resolution compared to existing millimetre arrays. Observations with ALMA will allow us to probe the nearby star forming regions discussed in this chapter on spatial scales of a few tens of AU, while allowing these types of analyses to be extended to the more distant regions of high mass star formation.

ALMA's broad wavelength coverage and flexible spectrometer will allow detailed studies of cores throughout the submillimetre windows, while its dual polarization receivers will allow sensitive high resolution observations of magnetic field signatures, both with polarization and with Zeeman observations.

Perhaps these instrumental advances will have helped to answer some of the questions raised in this chapter in time for PPVI.

REFERENCES

Aikawa Y., Herbst E., Roberts H., and Caselli P. (2005) *Astrophys. J., 620*, 330-346.

André P., Ward-Thompson D., and Barsony M. (1993) *Astrophys. J., 406*, 122-141.

André P., Ward-Thompson D., and Barsony M. (2000) In *Protostars and Planets IV* (V. Mannings, A. P. Boss, and S. S. Russell, eds.), pp. 59-96. Univ. of Arizona, Tucson.

André P., Belloche A., Motte F., and Peretto N. (2006) *Astron. Astrophys.*, in press.

Aoyama H., Mizuno N., Yamamoto H., Onishi T., Mizuno A., and Fukui Y. (2001) *Publ. Astron. Soc. Japan, 53*, 1053-1062.

Aso Y., Tatematsu K., Sekimoto Y., Nakano T., Umemoto T., et al. (2000) *Astrophys. J. Suppl., 131*, 465-482.

Ballesteros-Paredes J., Klessen R. S., and Vazquez-Semadeni E. (2003) *Astrophys. J., 592*, 188-202.

Basu S. (2000) *Astrophys. J., 540*, L103-106.

Basu S. and Mouschovias T. Ch. (1994) *Astrophys. J., 432*, 720-741.

Bate M. R., Bonnell I. A., and Bromm V. (2003) *Mon. Not. R. Astron. Soc., 339*, 577-599.

Beichman C. A., Myers P. C., Emerson J. P., Harris S., Mathieu R., Benson P. J., Jennings R. E. (1986) *Astrophys. J., 307*, 337-349.

Belloche A., André P., and Motte F. (2001) In *From Darkness to Light* (T. Montmerle and P. André, eds.), pp. 313-318, ASP, San Francisco.

Belloche A., André P., Despois D., and Blinder S. (2002) *Astron. Astrophys., 393*, 927-947.

Benson P. J. and Myers P. C. (1989) *Astrophys. J. Suppl., 71*, 89-108.

Beuther H. and Schilke P. (2004) *Science, 303*, 1167-1169.

Bonnell I. A., Bate M. R., Clarke C. J., and Pringle J. E. (2001) *Mon. Not. R. Astron. Soc., 323*, 785-794.

Bonnell I. A., Bate M. R., and Vine S. G. (2003) *Mon. Not. R. Astron. Soc., 343*, 413-418.

Bontemps S., André P., Kaas A. A., Nordh L., Olofsson G., et al. (2001) *Astron. Astrophys., 372*, 173-194.

Boss A. P. (1995) *Astrophys. J., 439*, 224-236.

Bourke T. L., Hyland A. R., and Robinson G. (1995a) *Mon. Not. R. Astron. Soc., 276*, 1052-1066.

Bourke T. L., Hyland A. R., Robinson G., James S. D., and Wright C. M. (1995b) *Mon. Not. R. Astron. Soc., 276*, 1067-1084.

Bourke T. L., Crapsi A., Myers P. C., Evans N. J., Wilner D. J., et al. (2005) *Astrophys. J., 633*, L129-132.

Caselli P., Benson P. J., Myers P. C., and Tafalla M. (2002) *Astrophys. J., 572*, 238-263.

Ceccarelli C., Castets A., Caux E., Hollenbach D., Loinard L., et al. (2000) *Astron. Astrophys., 355*, 1129-1137.

Chabrier G. (2003) *Publ. Astron. Soc. Pac., 115*, 763-795.

Chandler C. J. and Richer, J. S. (2000) *Astrophys. J., 530*, 851-866.

Chandrasekhar S. and Fermi E. (1953) *Astrophys. J., 118*, 113-115.

Ciolek G. E. and Basu S. (2001) *Astrophys. J., 547*, 272-279.

Clemens D. P. and Barvainis R. (1988) *Astrophys. J., Suppl., 68*, 257-286.

Crutcher R. M. (1999) *Astrophys. J., 520*, 706-713.

Crutcher R. M. and Troland T. H. (2000) *Astrophys. J., 537*, L139-L142.

Crutcher R. M., Troland T. H., Goodman A. A., Heiles C., Kazés I. and Myers P. C. (1993) *Astrophys. J., 407*, 175-184.

Crutcher R. M., Nutter D., Ward-Thompson D., and Kirk J. M. (2004) *Astrophys. J., 600*, 279-285.

Di Francesco J., Myers P. C., Wilner D. J., and Ohashi N. (2001) *Astrophys. J., 562*, 770-789.

Elmegreen B. G. (2000) *Astrophys. J., 530*, 277-281.

Enoch M. L., Young K. E., Glenn J., Evans N. J., Golwala S., et al. (2006) *Astrophys. J.*, in press.

Foster P. N. and Chevalier R. A. (1993) *Astrophys. J., 416*, 303-311.

Gammie C. F., Lin Y., Stone J. M., and Ostriker E. C. (2003) *Astrophys. J., 592*, 203-216.

Goldsmith P. F. and Li D. (2005) *Astrophys. J., 622*, 938-958.

Goodwin S. P., Whitworth A. P., and Ward-Thompson D. (2004) *Astron. Astrophys., 423*, 169-182.

Greene T. P., Wilking B. A., André P., Young E. T., and Lada C. J. (1994) *Astrophys. J., 434*, 614-626.

Gregersen E. M. and Evans N. J. (2000) *Astrophys. J., 538*, 260-267.

Hartmann L., Ballesteros-Paredes J., and Bergin E. A. (2001) *Astrophys. J., 562*, 852-868.

Heiles C. and Crutcher R. M. (2005) In *Cosmic Magnetic Fields, LNP 664*, (R. Wielebinski and R. Beck, eds.) pp. 137-183. Springer, Heidelberg.

Hennebelle P., Whitworth A. P., Gladwin P. P., and André P. (2003) *Mon. Not. R. Astron. Soc., 340*, 870-882.

Hennebelle P., Whitworth A. P., Cha S., and Goodwin S., (2004) *Mon. Not. R. Astron. Soc., 348*, 687-701.

Henriksen R., André P., and Bontemps S. (1997) *Astron. Astrophys., 323*, 549-565.

Hirano N., Ohashi N., and Dobashi K. (2002) In *8th Asian-Pacific Regional Meeting* (S. Ikeuchi, J. Hearnshaw, and T. Hanawa, eds.), pp. 141-142. Ast. Soc. Japan, Tokyo.

Hogerheijde M. R. and Sandell G. (2000) *Astrophys. J., 534*, 880-893.

Holland W. S., Robson E. I., Gear W. K., Cunningham C. R., Lightfoot J. F., et al. (1999) *Mon. Not. R. Astron. Soc., 303*, 659-672.

Jessop N. E. and Ward-Thompson D. (2000) *Mon. Not. R. Astron. Soc., 311*, 63-74.

Jijina J., Myers P. C., and Adams F. C. (1999) *Astrophys. J., Suppl., 125*, 161-236.

Johnstone D., Wilson C. D. Moriarty-Schieven G., Joncas G., Smith G., Gregersen E., and Fich, M. (2000) *Astrophys. J., 545*, 327-339.

Johnstone D., Fich M., Mitchell G. F., and Moriarty-Schieven G. (2001) *Astrophys. J., 559*, 307-317.

Johnstone D., Di Francesco J., and Kirk H. (2004) *Astrophys. J., 611*, L45-48.

Johnstone D., Matthews H., and Mitchell G. F. (2006) Astrophys. J., in press.

Kaas A. A., Olofsson G., Bontemps S., André P., Nordh L., et al. (2004) *Astron. Astrophys., 421*, 623-642.

Kandori R., Nakajima Y., Tamura M., Tatematsu K., Aikawa Y., *et al.* (2005) *Astron. J., 130*, 2166-2184.

Kenyon S. J. and Hartmann L. (1995) *Astrophys. J. Suppl., 101*, 117-171.

Kirk H. (2005) *MSc thesis*, University of Victoria, Canada.

Kirk H., Johnstone D., and Di Francesco J. (2006) *Astrophys. J.*, in press

Kirk J. M., Ward-Thompson D., and André P. (2005) *Mon. Not. R. Astron. Soc., 360*, 1506-1526.

Kirk J. M., Ward-Thompson D., and Crutcher R. M. (2006) *Mon. Not. R. Astron. Soc.*, in press.

Klessen R. S. (2001a) *Astrophys. J., 550*, L77-80.

Klessen R. S. (2001b) *Astrophys. J., 556*, 837-846.

Klessen R. S. and Burkert A. (2000) *Astrophys. J. Suppl., 128*, 287-319.

Klessen R. S., Burkert A., and Bate M. R. (1998) *Astrophys. J., 501*, L205-208.

Kreysa E., Gemuend H. P., Gromke J., Haslam C. G., Reichertz L., et al. (1999) *Soc. Phot. Inst. Eng., 3357*, 319-325.

Kroupa P. (2002) *Science, 295*, 82-91.

Kulsrud R. and Pearce W. P. (1969) *Astrophys. J., 156*, 445-469.

Lada C. (1987) In *Star Forming Regions* (M. Peimbert and J. Jugaku, eds.), pp. 1-17. Reidel, Dordrecht.

Larson R. B. (1981) *Mon. Not. R. Astron. Soc., 194*, 809-826.

Lee C. W. and Myers P. C. (1999) *Astrophys. J. Suppl., 123*, 233-250.

Lee C. W., Myers P. C., and Tafalla M. (1999) *Astrophys. J., 526*, 788-805.

Looney L. W., Mundy L. G., and Welch W. J. (2003) *Astrophys. J., 592*, 255-265.

Loren R. B. (1989) *Astrophys. J., 338*, 902-924.

MacLow M.-M. and Klessen R. S. (2004) *Rev. Mod. Phys., 76*, 125-194.

MacLow M.-M., Klessen R. S., Burkert A., and Smith M. D. (1998) *Phys. Rev. Lett., 80*, 2754-2757.

Maret S., Ceccarelli C., Caux E., Tielens A. G. G. M., and Castets A. (2002) *Astron. Astrophys., 395*, 573-585.

Matthews B. C. and Wilson C. D. (2002) *Astrophys. J, 574*, 822-833.

Matthews B. C., Wilson C. D., and Fiege J. D. (2001) *Astrophys. J, 562*, 400-423.

McKee C. F. (1989) *Astrophys. J, 345*, 782-801.

McKee C. F. and Tan J. (2003) *Astrophys. J., 585*, 850-871.

Mookerjea B., Kramer C., Nielbock M., and Nyman L. A. (2004) *Astron. Astrophys., 426*, 119-129.

Motoyama K. and Yoshida T. (2003) *Mon. Not. R. Astron. Soc., 344*, 461-467.

Motte F. and André P. (2001) *Astron. Astrophys., 365*, 440-464.

Motte F., André P., and Neri R. (1998) *Astron. Astrophys., 336*, 150-172.

Motte F., André P., Ward-Thompson D., and Bontemps S. (2001) *Astron. Astrophys., 372*, L41-44.

Motte F., Schilke P., and Lis D. C. (2003) *Astrophys. J., 582*, 277-291.

Mouschovias T. Ch. (1991) *Astrophys. J., 373*, 169-186.

Mouschovias T. Ch. and Ciolek G. E. (1999) In *The Origin of Stars and Planetary Systems* (C. J. Lada and N. D. Kylafis,

eds.), pp. 305-339. Kluwer, Dordrecht.

Mouschovias T. Ch., Tassis K., and Kunz M. W. (2006) *Astrophys. J.*, in press.

Myers P. C. (1998) *Astrophys. J., 496*, L109-112.

Myers P. C. (2000) *Astrophys. J., 530*, L119-122.

Myers P. C., Linke R. A., and Benson P. J. (1983) *Astrophys. J, 264*, 517-537.

Nakano T. (1998) *Astrophys. J., 494*, 587-604.

Nutter D. J., 2004, *PhD Thesis*, Cardiff University.

Nutter D. J., Ward-Thompson D., and André P. (2006) *Mon. Not. R. Astron. Soc.,* in press.

Ohashi N. (1999) In *Star Formation 1999* (T. Nakamoto, ed.), pp. 129-135. Nobeyama Radio Obser., Nobeyama.

Onishi T., Mizuno A., Kawamura A., Ogawa H., and Fukui Y. (1998) *Astrophys. J, 502*, 296-314.

Onishi T., Kawamura A., Abe R., Yamaguchi N., Saito H., et al. (1999) *Publ. Astron. Soc. Japan,* 51, 871-881.

Onishi T., Mizuno A., Kawamura A., Tachihara K., and Fukui Y. (2002) *Astrophys. J., 575*, 950-973.

Ostriker E. C., Gammie C. F., and Stone J. M. (1999) *Astrophys. J, 513*, 259-274.

Padoan P. and Nordlund A. (2002) *Astrophys. J., 576*, 870-879.

Parker E. N. (1966) *Astrophys. J., 145*, 811-833.

Peretto N., André P., and Belloche A. (2006) *Astron. Astrophys., 445*, 979-998.

Reid M. A. (2005) *Ph.D. thesis,* McMaster University, Canada.

Reid M. A. and Wilson C. D. (2005) *Astrophys. J., 625*, 891-905.

Reid M. A. and Wilson C. D. (2006) *Astrophys. J.,* in press.

Salpeter E. E. (1955) *Astrophys. J., 121*, 161-167.

Schmeja S. and Klessen R. S. (2004) *Astron. Astrophys., 419*, 405-417.

Shirley Y. L., Evans N. J., Rawlings J. M. C., and Gregersen E. M. (2000) *Astrophys. J., Suppl., 131*, 249-271.

Shirley Y. L., Evans N. J., Young K. E., Knez C., and Jaffe D. T. (2003) *Astrophys. J. Suppl., 149*, 375-403.

Shu F. H., Adams F. C., and Lizano S. (1987) *Ann. Rev. Astron. Astrophys., 25*, 23-81.

Stanke T., Smith M. D., Gredel R., and Khanzadyan T. (2006) *Astron. Astrophys.*, in press.

Tachihara K., Mizuno A., and Fukui Y. (2000) *Astrophys. J., 528*, 817-840.

Tachihara K., Onishi T., Mizuno A., and Fukui Y. (2002) *Astron. Astrophys., 385*, 909-920.

Tafalla M., Mardones D., Myers P. C., Caselli P., Bachiller R. and Benson P. J. (1998) *Astrophys. J., 504*, 900-914.

Tassis K. and Mouschovias T. Ch. (2004) *Astrophys. J., 616*, 283-287.

Tatematsu K., Umemoto T., Kandori R., and Sekimoto Y. (2004) *Astrophys. J., 606*, 333-340.

Testi L. and Sargent A. I. (1998) *Astrophys. J., 508*, L91-94.

Tilley D. and Pudritz R. E. (2004) *Mon. Not. R. Astron. Soc., 353*, 769-788.

Tothill N. F. H., White G. J., Matthews H. E., McCutcheon W. H., McCaughrean M. J., and Kenworthy M. A. (2002) *Astrophys. J., 580*, 285-304.

Vazquez-Semadeni E., Kim J., Shadmehri M., and Ballesteros-Paredes J. (2005) *Astrophys. J., 618*, 344-359.

Walsh A. J., Myers P. C., and Burton M. G. (2004) *Astrophys. J, 614*, 194-202.

Ward-Thompson D. (2002) *Science, 295*, 76-81.

Ward-Thompson D. and Buckley H. D. (2001) *Mon. Not. R. Astron. Soc.,* 327, 955-983.

Ward-Thompson D., Scott P. F., Hills R. E., and André P. (1994) *Mon. Not. R. Astron. Soc., 268*, 276-290.

Ward-Thompson D., Motte F., and André P. (1999) *Mon. Not. R. Astron. Soc., 305*, 143-150.

Ward-Thompson D., Kirk J. M., Crutcher R. M., Greaves J. S., Holland W. S., and André P. (2000) *Astrophys. J., 537*, L135-L138.

Whitworth A. P. and Summers D. (1985) *Mon. Not. R. Astron. Soc., 214*, 1-25.

Whitworth A. P. and Ward-Thompson D. (2001) *Astrophys. J., 547*, 317-322.

Wilking B. A., Lada C. J., and Young E. T. (1989) *Astrophys. J., 340*, 823-852.

Williams J. P., Myers P. C., Wilner D. J., and Di Francesco J. (1999) *Astrophys. J., 513*, L61-L64.

Wolf S., Launhardt R., and Henning T. (2003) *Astrophys. J., 592*, 233-244.

Wood D. O. S., Myers P. C., and Daugherty D. A. (1994) *Astrophys. J. Suppl., 95*, 457-501.

Young C. H., Jorgensen J. K., Shirley Y. L., Kauffmann J., Huard T., *et al.* (2004) *Astrophys. J. Suppl., 154*, 396-401.